Astronomy & Astrophysics manuscript no. AA24283accepted
June 24, 2014
©ESO 2014

arXiv:1406.5578v1 [astro-ph.CO] 21 Jun 2014

Tracing high redshift cosmic web with quasar systems

Maret Einasto[1], Erik Tago[1], Heidi Lietzen[1, 2, 3], Changbom Park[4], Pekka Heinämäki[5], Enn Saar[1, 6], Hyunmi Song[4], Lauri Juhan Liivamägi[1, 7], and Jaan Einasto[1, 6, 8]

[1] Tartu Observatory, 61602 Tõravere, Estonia
[2] Instituto de Astrofísica de Canarias, E-38205 La Laguna, Tenerife, Spain
[3] Universidad de La Laguna, Dept. Astrofísica, E-38206 La Laguna, Tenerife, Spain
[4] School of Physics, Korea Institute for Advanced Study, 85 Hoegiro, Dong-Dae-Mun-Gu, Seoul 130-722, Korea
[5] Tuorla Observatory, University of Turku, Väisäläntie 20, Piikkiö, Finland
[6] Estonian Academy of Sciences, EE-10130 Tallinn, Estonia
[7] Institute of Physics, Tartu University, Tähe 4, 51010 Tartu, Estonia
[8] ICRANet, Piazza della Repubblica 10, 65122 Pescara, Italy

Received / Accepted

ABSTRACT

Context. To understand the formation, evolution, and present-day properties of the cosmic web we need to study it at low and high redshifts.
Aims. We trace the cosmic web at redshifts $1.0 \leq z \leq 1.8$ using the quasar (QSO) data from the SDSS DR7 QSO catalogue (Schneider et al. 2010).
Methods. We apply a friend-of-friend (FoF) algorithm to the quasar and random catalogues to determine systems at a series of linking lengths, and analyse richness and sizes of these systems.
Results. At the linking lengths $l \leq 30\ h^{-1}$ Mpc the number of quasar systems is larger than the number of systems detected in random catalogues, and systems themselves have smaller diameters than random systems. The diameters of quasar systems are comparable to the sizes of poor galaxy superclusters in the local Universe, the richest quasar systems have four members. The mean space density of quasar systems, $\approx 10^{-7}(\mathrm{h^{-1}Mpc})^{-3}$, is close to the mean space density of local rich superclusters. At intermediate linking lengths ($40 \leq l \leq 70\ h^{-1}$ Mpc) the richness and length of quasar systems are similar to those derived from random catalogues. Quasar system diameters are similar to the sizes of rich superclusters and supercluster chains in the local Universe. The percolating system which penetrate the whole sample volume appears in quasar sample at smaller linking length than in random samples ($85\ h^{-1}$ Mpc). At the linking length $70\ h^{-1}$ Mpc the richest systems of quasars have diameters exceeding $500\ h^{-1}$ Mpc, three systems in our catalogue are the same as described in Clowes et al. (2012, 2013). Quasar luminosities in systems are not correlated with the system richness.
Conclusions. Quasar system catalogues at our web pages serve as a database to search for superclusters of galaxies and to trace the cosmic web at high redshifts.

Key words. Cosmology: large-scale structure of the Universe; quasars: general

1. Introduction

Contemporary cosmological paradigm tells us that the structure in the Universe–the cosmic web formed and evolved from tiny density perturbations in the very early Universe by hierarchical growth driven by gravity (see, e.g., Loeb 2008; van de Weygaert & Schaap 2009, and references therein). Groups and clusters of galaxies and their filaments formed by density perturbations of scale up to 32 h^{-1} Mpc, superclusters of galaxies, the largest density enhancements in the local cosmic web, by larger-scale perturbations, up to 100 h^{-1} Mpc. Still larger-scale density perturbations modulate the richness of galaxy systems (Einasto et al. 2011a; Suhhonenko et al. 2011).

To understand how the cosmic web formed and evolved it is of paramount importance to describe and quantify it at low and high redshifts. Large galaxy redshift surveys like SDSS enable us to describe the cosmic web in our neighbourhood in detail. One source of information about the cosmic structures at high redshifts is the distribution of quasars. Quasars lie at centres of massive galaxies (Hutchings et al. 2002; Kotilainen et al. 2009; Padmanabhan et al. 2009; Letawe et al. 2010; Kotilainen et al. 2013; Falomo et al. 2013; Floyd et al. 2013; Falomo et al. 2014; Karhunen et al. 2014a, and references therein), being members of galaxy systems, usually small groups and poor clusters (Wold et al. 2000; Soechting et al. 2002; Söchting et al. 2004; Coldwell & Lambas 2006; Hutchings et al. 2009; Trainor & Steidel 2012; Ueda et al. 2013). Nearby quasars are typically located in a relatively low-density large-scale environment near superclusters of galaxies (Coldwell & Lambas 2006; Lietzen et al. 2009, 2011).

Galaxy luminosities, morphological types, colors, star formation rates, and other properties are closely related to their environment at small and large scales (Einasto et al. 1974; Dressler 1980; Einasto & Einasto 1987; Mo et al. 1992; Park et al. 2007; Park & Choi 2009; Skibba 2009; Tempel et al. 2011; Lietzen et al. 2012; Einasto et al. 2014). The studies of quasar environment in the cosmic web helps us to understand the relation between galaxy and quasar evolution and to test the evolutionary schemes of different type of objects.

Already decades ago several studies described large systems in quasar distribution (Webster 1982; Clowes & Campusano

Send offprint requests to: M. Einasto

1991; Komberg et al. 1996; Williger et al. 2002; Clowes et al. 2012, 2013, and references therein) which are known as Large Quasar Groups (LQGs). Miller et al. (2004) found significant 200 h^{-1} Mpc size over- and underdensities in the density field determined by quasars from 2dF QSO Redshift survey. LQGs may trace distant galaxy superclusters (Komberg et al. 1996). The large-scale distribution of quasar systems gives us information about the cosmic web at high redshifts which are not yet covered by large and wide galaxy surveys.

The goal of this study is to analyse the distribution of quasars at redshifts $1.0 \leq z \leq 1.8$. We choose this redshift range as we are interested in the study of the cosmic web at high redshifts. This redshift range was also used by Clowes et al. (2012, 2013); with this choice we can compare LQGs found in these studies, and our systems. We shall use Schneider et al. (2010) catalogue of quasars, based on the Sloan Digital Sky Survey Data Release 7 (SDSS DR7). We analyse clustering properties of quasars with the FoF algorithm, compare them with random distributions, and determine systems of quasars at a series of linking lengths. We present catalogues of quasar systems, and analyse their properties and large-scale distribution.

In Sect. 2 we describe the data we used and the method in Sect. 3. In Sect. 4 we give the results. We discuss the results in Sect. 5, and summarise the results in Sect. 5.3. In Appendix A we present data about the richest quasar systems.

At `http://www.aai.ee/~maret/QSOsystems.html` we present the quasar system catalogues. There we present also an interactive pdf file showing the distribution of quasar systems.

We assume the standard cosmological parameters: the Hubble parameter $H_0 = 100\ h$ km s^{-1} Mpc^{-1}, the matter density $\Omega_{\rm m} = 0.27$, and the dark energy density $\Omega_\Lambda = 0.73$.

2. Data

We adopt a catalogue of quasars with a spectrum taken as a normal science spectrum (SCIENCEPRIMARY=1) and a photometric measurement designated PRIMARY in the BEST photometric database. We select from this catalogue a subsample of quasars in the redshift interval $1.0 \leq z \leq 1.8$, and apply i-magnitude limit $i = 19.1$. The full quasar catalogue by Schneider et al. (2010) is not homogeneous; Vanden Berk et al. (2005); Richards et al. (2006) (see also Clowes et al. 2012) gave a detailed analysis of the completeness of the sample and suggested to use these selection limits for statistical studies. In order to reduce the edge effects of our analysis, we limit the data in the area of SDSS sky coordinate limits $-55 \leq \lambda \leq 55$ degrees and $-33 \leq \eta \leq 35$ degrees. Our final sample contains data of 22381 quasars.

In Fig. 1 we plot the number density of quasars at different distances. The mean space density of quasars is approximately $1.1 \cdot 10^{-6}(\mathrm{h}^{-1}\mathrm{Mpc})^{-3}$. The density decreases slightly with distance. Below we analyse whether this trend affects the result of our analysis. Figure 1 demonstrates several wiggles in the number density of quasars which correspond to the location of very rich quasar systems, as we show below.

The space density of quasars is very low, therefore it is important to understand whether their distribution differs from random distribution. To compare quasar and random distributions we generated random samples using the same coordinate λ, η and redshift limits as quasar samples. The number of random points in random samples was equal to the number of quasars.

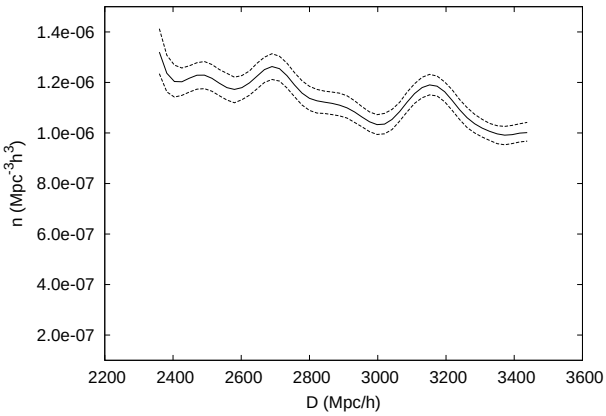

Fig. 1. Quasar number density versus distance. Dotted lines show the 98% central confidence limits.

3. Method

We employed the Friends-of-Friends (FoF) clustering analysis method introduced in cosmology by Zeldovich et al. (1982) and Huchra & Geller (1982) to determine systems in the quasar catalogue and random catalogues. FoF method is commonly used to detect groups and clusters in the galaxy distribution (Tucker et al. 2000; Eke et al. 2004; Tago et al. 2006, 2008; Park et al. 2012; Tempel et al. 2012, 2014, and references therein), and superclusters of optical and X-ray clusters of galaxies (Einasto et al. 1994, 2001; Chon et al. 2013). Komberg et al. (1996) applied FoF method to search for rich quasar systems.

FoF method collects objects into systems if they have at least one common neighbour closer than a linking length. At small linking lengths l only the closest neighbouring objects form systems, most objects in the sample remain single. As the linking length increases more and more objects join systems, and the number of systems, their richness and size increase. At a certain linking length the largest system spans over the whole sample volume–a percolation occurs. We apply FoF algorithm to quasar and random samples with a series of linking lengths to analyse the properties of systems and their percolation. Klypin & Shandarin (1993) showed that the richness and size of the richest and 2nd richest system in a sample characterise well the growth of systems and percolation properties of a sample. Therefore we analyse the properties of the richest systems in quasar and random catalogues at each linking length.

4. Results

4.1. FoF analysis

The FoF algorithm was applied to observed quasar and random catalogues at a series of linking lengths. At each linking length we found the number of systems in quasar and random samples with at least two members, calculated multiplicity functions of systems, and found the length and size of the first and second largest system. In Tables A.1, A.2, and A.3 we present the data about the richest systems of quasars at linking lengths 20, 30, and 70 h^{-1} Mpc.

Figure 2 shows the number of systems from the quasar and random catalogues (upper panel), and the ratio of the numbers of systems (lower panel). At the linking lengths up to approximately 50 h^{-1} Mpc the number of quasar systems is larger than the number of systems in random catalogues. At higher values of the linking lengths the number of systems in quasar catalogue

becomes similar to that in random catalogue. The number of systems in both quasar and random catalogues reaches maximum at 60 h^{-1} Mpc. At higher values of the linking lengths systems begin to join into larger systems and the number of systems decreases.

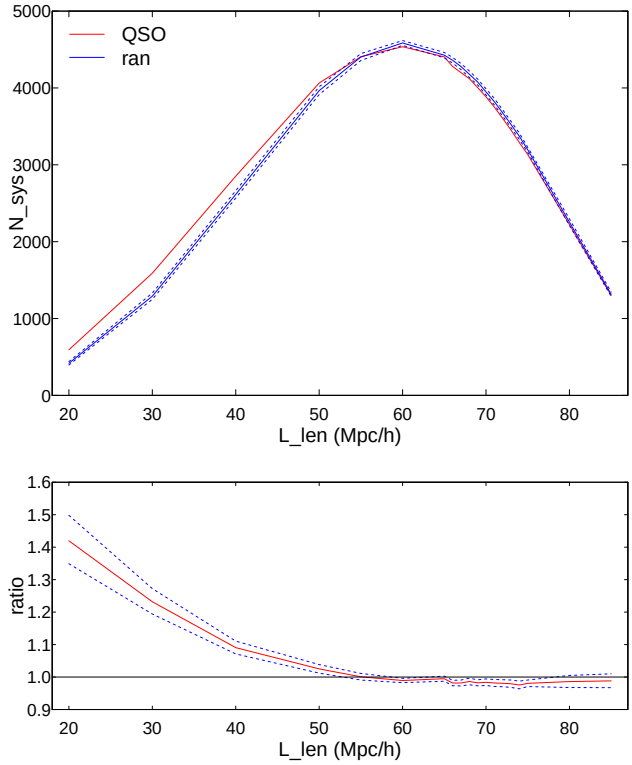

Fig. 2. The number of quasar and random systems (upper panel) and the ratio of the numbers of quasar and random systems (lower panel) vs. the linking length. Red solid line denote quasar systems, and blue lines denote random systems, black line shows ratio 1.

The richness and diameters (maximum distance between quasar pairs in a system) of the largest two systems in quasar and random catalogues is given in Table 1. Table 1 show that at the linking lengths $l \leq 30\ h^{-1}$ Mpc the richest quasar systems have smaller diameters than the richest random systems. In a wide linking length interval, $40 \leq l \leq 70\ h^{-1}$ Mpc, the richness and diameters of the richest quasar systems are comparable to those found in random catalogues. At the linking length 80 h^{-1} Mpc quasar systems start to join, the richness and diameter of the richest quasar system increase rapidly. The increase of the richness and size of the richest random system is much smaller. At the linking length $l = 85\ h^{-1}$ Mpc about half of quasars join the richest quasar system– a percolation occurs. The richness and diameter of the richest system in random catalogues also increase, being still poorer than the richest system in the quasar catalogue. The second richest system in random catalogues is much richer than the second richest system in quasar catalogue. This shows that the percolation of quasar and random systems occurs differently, and the properties of the richest systems differ.

We also analysed the multiplicity functions which show the fractions of systems of different richness in quasar and random samples at a series of linking lengths. Up to the linking length $l = 70\ h^{-1}$ Mpc the multiplicity functions for quasar and random catalogues are very similar. At the linking length 80 h^{-1} Mpc the richness of the richest quasar system increases rapidly - systems start to join into one huge percolating system, as we showed above, and multiplicity functions of quasars and random systems

Table 1. The number of objects in the two richest systems, and system diameters from quasar and random catalogues at a series of linking lengths

(1)	(2)	(3)	(4)	(5)
l	$N1_{QSO}$	$N1_{ran}$	$D1_{QSO}$	$D1_{ran}$
20	3	3.3± 0.5	31.0	33.5 ± 2.0
30	4	4.9± 0.8	58.8	70.0 ± 5.2
40	7	7.6± 1.3	109.4	119.2 ± 17.4
50	15	12.3± 2.2	178.6	209.7 ± 14.7
60	23	21.3± 2.0	324.9	369.8 ± 40.1
70	67	65.1± 11.7	703.1	717.1 ± 86.0
75	105	146.3± 39.9	865.3	992.5 ± 145.9
80	920	460.0± 54.1	2066.4	1750.2 ± 171.1
85	11415	6464.0± 1886.3	5060.3	4552.7 ± 645.4
l	$N2_{QSO}$	$N2_{ran}$	$D2_{QSO}$	$D2_{ran}$
20	3	2.3 ± 0.5	29.9	30.9 ± 2.6
30	4	3.7 ± 0.5	49.4	61.4 ± 3.6
40	7	6.0 ± 0.9	106.8	104.3 ± 4.9
50	14	10.6 ± 1.5	177.7	185.6 ± 16.3
60	20	19.9 ± 1.9	294.0	307.0 ± 29.3
70	64	56.3 ± 7.8	614.6	626.2 ± 46.9
75	97	109.1 ± 24.9	792.3	883.5 ± 53.8
80	421	372.4 ± 71.3	1832.7	1539.5 ±143.0
85	678	2652.3 ± 859.1	1789.1	2337.6 ±782.2

Notes. Columns are as follows: 1: linking length l in h^{-1} Mpc; 2: the number of quasars in the 1st and 2nd richest quasar system; 3: mean number of random points in the 1st and 2nd richest quasar system; 4: the diameter of the 1st and the 2nd richest quasar system in h^{-1} Mpc; 5: the diameter of the 1st and the 2nd richest random system in h^{-1} Mpc.

become different. The differences are the largest at the linking length 85 h^{-1} Mpc.

Next we compare the distribution of diameters of quasar and random systems. We show in Fig. 3 the numbers of quasar and random systems of different diameter at the linking lengths 30 and 70 h^{-1} Mpc. At the linking length 20 h^{-1} Mpc the diameters of the triple quasar systems are given in Table A.1.

At the linking lengths 20 and 30 h^{-1} Mpc most systems in both quasar and random catalogues are pairs, the richest systems have four (three at $l = 20\ h^{-1}$ Mpc) members. The diameters of the quasar pairs are as small as 5 h^{-1} Mpc in the closest pairs, the number of close pairs of quasars is larger than the number of close random points. The lengths of the quasar systems are up to about 30 – 40 h^{-1} Mpc, the highest values of diameters are up to 60 h^{-1} Mpc. In the whole diameter interval the number of quasar systems with a given diameter is higher than that of random systems (except the highest values of diameters; the number of systems with diameters larger than 50 h^{-1} Mpc is higher among random systems), the differences are the largest up to diameters 20 h^{-1} Mpc.

At larger linking lengths ($l \geq 40\ h^{-1}$ Mpc; we show this for 70 h^{-1} Mpc) the number of quasar systems with diameters up to 20 h^{-1} Mpc is always larger than the number of random systems at these diameters. These systems are mostly pairs, but there are also richer systems among them. Starting from diameters $\approx$ 30 h^{-1} Mpc the number of systems of different diameter in quasar and random catalogues becomes similar.

The Kolmogorov-Smirnov (KS) test shows that the differences of the distributions of system sizes at the linking lengths 20 and 30 h^{-1} Mpc between quasar and random samples are

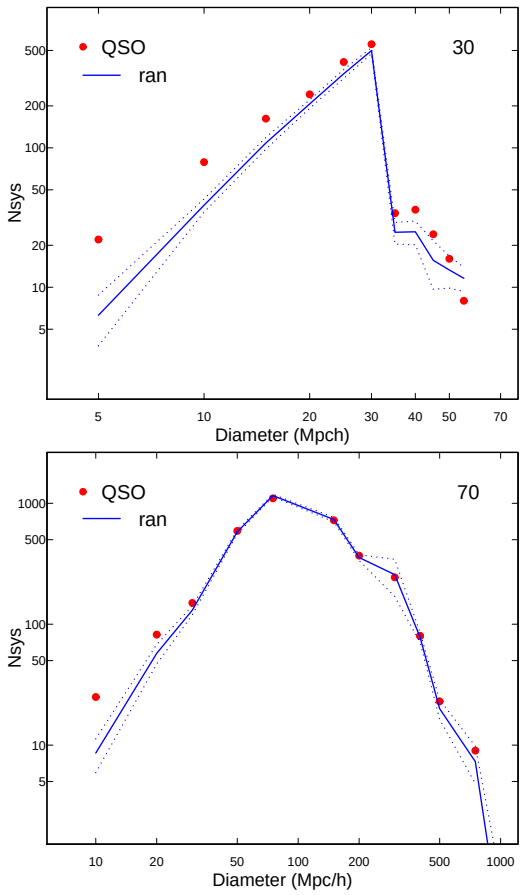

Fig. 3. Number of quasar (red dots) and random (blue lines) systems of different diameter for linking lengths 30 and 70 h^{-1} Mpc (upper and lower panel, correspondingly).

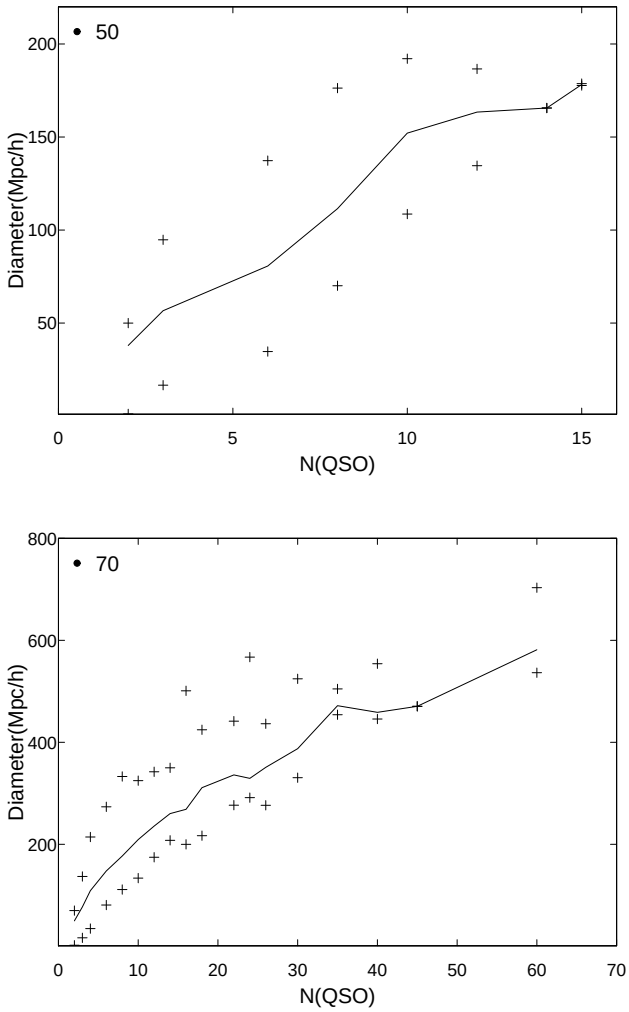

Fig. 4. System richness N_{QSO} vs. their diameter D_{max} for quasars for linking lengths 50 and 70 h^{-1} Mpc. Lines show median values of diameters, crosses denote the smallest and the largest diameters.

statistically highly significant ($p_{KS} < 0.003$). At higher values of the linking lengths the sizes of quasar systems with at least three members are statistically similar to those found in random samples; the diameters of quasar pairs are at all linking lengths smaller than diameters of pairs from random catalogues, and these differences are statistically highly significant ($p_{KS} < 0.05$).

Therefore the FoF analysis reveals that we obtain catalogues of real quasar systems in which the number of systems and system diameters differ from those found in random catalogues at linking lengths $l \leq 30$, there is relatively more close pairs among quasars than in random catalogues. This causes also stronger correlation of quasars than random catalogues at small scales (Shen et al. 2007; Mountrichas et al. 2009; Donoso et al. 2010; Shen et al. 2013).

4.2. Properties of quasar systems.

In Fig. 4 we show the median, and minimum and maximum values of quasar system diameters vs. their richness at the linking lengths 50 and 70 h^{-1} Mpc. At the linking lengths 20 and 30 h^{-1} Mpc we give the sizes of the largest systems in Tables A.1 and A.2.

At the linking lengths 20 and 30 h^{-1} Mpc the sizes of quasar systems, up to 30 – 60 h^{-1} Mpc, are comparable with the sizes of poor and medium rich galaxy superclusters in the local universe (Einasto et al. 1994, 1997; Jaaniste et al. 1998) with the number of Abell clusters $N_{cl} < 8$. At the linking lengths 40 and 50 h^{-1} Mpc the richest quasar systems have up to 15 members. The sizes of the richest quasar systems, $\approx 200\,h^{-1}$ Mpc, are comparable to the sizes of the richest superclusters and supercluster chains in the local universe, typically containing 15–20 rich (Abell) galaxy clusters (Jaaniste et al. 1998; Einasto et al. 1994; Costa-Duarte et al. 2011; Schirmer et al. 2011; Liivamägi et al. 2012; Chon et al. 2013). The mean space density of quasar systems at these linking lengths is of order of $10^{-7}(\mathrm{h}^{-1}\mathrm{Mpc})^{-3}$, this is close to the mean space density of rich superclusters of Abell clusters with at least 10 member clusters (Einasto et al. 1997). The similarity of the mean space density of quasar systems and local rich superclusters was noted already by Komberg et al. (1996).

At the linking length $l = 70\ h^{-1}$ Mpc rich quasar systems with at least 30 member quasars and size at least 300 h^{-1} Mpc (22 systems, Table A.3) are comparable in size with those described in Park et al. (2012) and in Luparello et al. (2011) as the richest systems in the local universe. The sizes of the largest quasar systems at $l = 70\ h^{-1}$ Mpc, 500 – 700 h^{-1} Mpc, are comparable with the sizes of supercluster complexes, in some cases penetrating the whole SDSS survey volume (Einasto et al. 2011c,b; Liivamägi et al. 2012). Einasto et al. (2011c) showed that the richest local supercluster complex, the Sloan Great Wall, consists of several rich superclusters. Individual superclusters in the Sloan Great Wall have different morphology and galaxy con-

tent, therefore they form an assembly of physically different systems.

We also analysed luminosities of quasars in systems of different richness and found that, in average, the luminosities of quasars in systems do not depend on system richness, the luminosities of quasars in systems, and those of single quasars are similar.

4.3. Individual quasar systems.

We show in Fig. 5 the distribution of quasars in systems of various richness at linking length 70 h^{-1} Mpc in cartesian coordinates x, y, and z defined as in Park et al. (2007) and in Liivamägi et al. (2012):

$$x = -d \sin\lambda,$$
$$y = d \cos\lambda \cos\eta,$$
$$z = d \cos\lambda \sin\eta,$$

where d is the comoving distance, and λ and η are the SDSS survey coordinates. We plot in the figure also quasars from the richest systems at $l = 20$ h^{-1} Mpc (quasar triplets). The richest quasar systems at $l = 20$ h^{-1} Mpc are almost all relatively isolated and do not belong to very rich quasar systems at higher linking lengths. This can be seen in Table A.1 where we give the richness of systems to which they belong at $l = 70$ h^{-1} Mpc. Table A.1 shows that triple quasar systems are located in two relatively narrow redshift intervals, at $z \approx 1.2$, and at $z \approx 1.7$.

In Fig. 5 and Table A.3 four systems at the linking length $l = 70$ h^{-1} Mpc consist of more than 50 quasars, and have diameters larger than 500 h^{-1} Mpc, exceeding the size of the richest local supercluster complex, the Sloan Great Wall. The richest system at the linking length $l = 70$ h^{-1} Mpc at $x \approx 1000$ h^{-1} Mpc and $y \approx 2500$ h^{-1} Mpc is the Huge-LQG described in Clowes et al. (2013). In our catalogue this system has 67 member quasars, and it is $\approx$ 700 h^{-1} Mpc in diameter. Below this system, at $y \approx 2000$ h^{-1} Mpc there are two quasar groups which coincide with those from Clowes et al. (2012).

Figure 6 shows the distribution of quasar systems at the linking length 80 h^{-1} Mpc. The members of the two largest systems are shown. This figure shows that the richest system form at $x < 0$ h^{-1} Mpc. This is the area where the space density of quasars at large scales is the highest. At this linking length the richest quasar systems found at $l = 70$ h^{-1} Mpc is a member of the second richest system.

4.4. Large-scale distribution of quasar systems

Visual inspection of Fig. 5 shows that in some areas of the figure there are underdense regions between rich quasar systems with diameters of about 400 h^{-1} Mpc (e.g. in the upper panel between $-1000 < x < 1000$ h^{-1} Mpc). The size of underdense regions in this figure is much larger than the sizes of typical large voids in the local Universe (Einasto et al. 2011a, and references therein) but is close to the sizes of the largest voids covered by SDSS survey (Einasto et al. 2011b; Park et al. 2012).

Miller et al. (2004) calculated the density field of quasars from 2dF QSO redshift survey and showed by visual inspection of the density field plots the presence of density fluctuations at scales of about 200 h^{-1} Mpc. We shall analyse the large scale distribution of quasar systems in detail in another study.

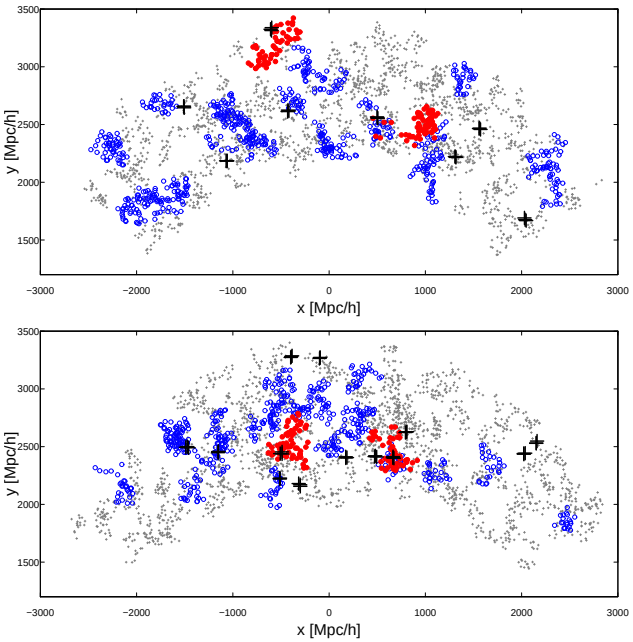

Fig. 5. Distribution of QSO systems at the linking length 70 h^{-1} Mpc in x and y coordinates in two slices by z coordinate (upper panel: $z \leq 0$ h^{-1} Mpc, lower panel: $z > 0$ h^{-1} Mpc). Grey dots denote quasars in systems with $10 \leq N_{QSO} \leq 24$, blue circles denote quasars in systems with $25 \leq N_{QSO} \leq 49$, and red filled circles denote quasars in systems with $N_{QSO} \geq 50$. Black crosses denote quasar triplets at a linking length 20 h^{-1} Mpc.

5. Discussion and conclusions

5.1. Selection effects

We analysed the diameters of systems at different distances to see whether the properties of quasar systems found with FoF method are affected by distance-dependent selection effects. Figure 7 shows the median diameters of quasar systems at the linking lengths 20–70 h^{-1} Mpc vs. their distances. The median diameters of quasar systems are not correlated with distance. We confirmed this also by correlation tests. We obtained similar results with systems from random catalogues. Apparent decrease of the median diameters of quasar systems at the linking length 70 h^{-1} Mpc at high distances is due to an edge effect–close to the sample boundaries FoF cannot find very large systems near sample edges. This edge effect is much stronger than the influence of the slight density decrease to the systems properties. Due to the edge effect we cannot search for quasar systems dividing volume under study into narrow slices–this might minimise other selection effects but makes the edge effects very strong. The edge effect affects quasar and random systems in the same way and may decrease the number of the largest quasar and random systems at large linking lengths. At the linking length 70 h^{-1} Mpc wiggles in the distribution of the system diameters are due to the largest quasar systems. These wiggles were also seen in Fig. 1.

Therefore the slight decrease of the number density of quasars with distance do not affect significantly the properties of quasar systems. It is possible that two effects cancel each other out - the possible increase of quasar systems due to the decrease of the density, and the decrease of systems due to cosmic evolution of systems at high redshift (Suhhonenko et al. 2011). We plan to study quasar and web evolution from simulations to understand better the evolutionary effects.

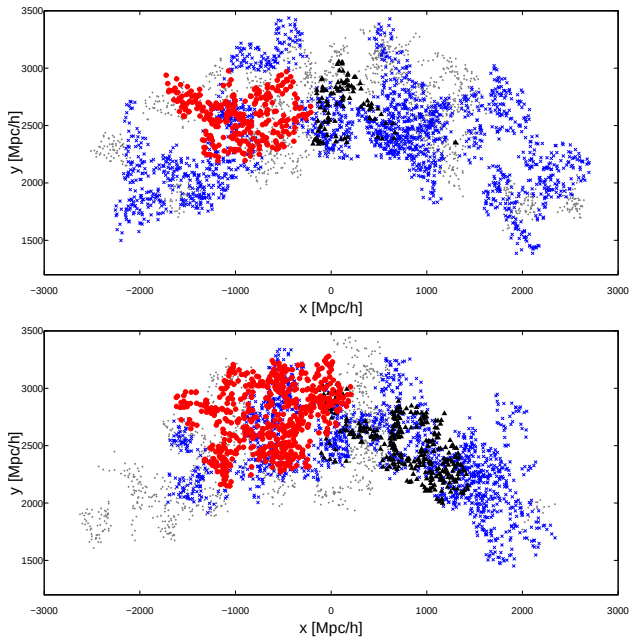

Fig. 6. Distribution of QSO systems at the linking length 80 h^{-1} Mpc in x and y coordinates in two slices by z coordinate (upper panel: $z \leq 0$ h^{-1} Mpc, lower panel: $z > 0$ h^{-1} Mpc). Grey dots denote quasars in systems with $50 \leq N_{QSO} < 100$, blue circles denote quasars in systems with $100 \leq N_{QSO} \leq 400$, black triangles denote quasars in the second richest system with $N_{QSO} = 421$ and red filled circles denote quasars in the richest system with $N_{QSO} = 920$.

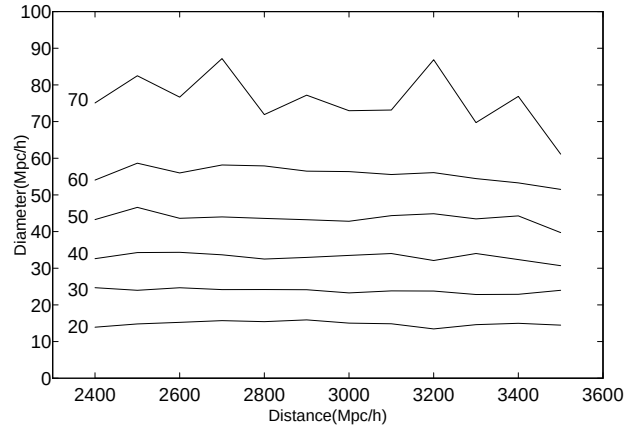

Fig. 7. Median diameters of quasar systems at linking lengths 20–70 h^{-1} Mpc vs. the distance of systems.

With SDSS Visual Tools we checked the images of selected quasars. We looked at images of all quasars in systems with more than two members at the linking lengths $l = 20$ and 30 h^{-1} Mpc, and in the richest systems at the linking length 70 h^{-1} Mpc, and did not detect contaminated images.

5.2. Discussion

We found that at the linking lengths $l \geq 40$ h^{-1} Mpc the number of quasar systems, their sizes and richness are comparable with sizes and richness of random systems, and therefore their presence do not violate homogeneity of the universe at very large scales, as claimed by Clowes et al. (2013). Similar conclusions were reached by Nadathur (2013). Transition scale to homogeneity has been discussed in many studies, see Einasto & Gramann (1993); Martinez et al. (1998) and Clowes et al. (2013) for details and references. Clowes et al. (2013) also mentioned that the richest quasar systems and therefore the highest large-scale density regions in the Universe are located in the area of the Huge-LQG. In our study we found several quasar systems comparable in richness with the Huge-LQG in other regions of space, where also the percolating systems appear. Therefore the Huge-LQG and other Large Quasar Groups near it form one of several complexes of rich quasar systems, and not the richest one.

At the linking length $l = 70$ h^{-1} Mpc the sizes of the largest quasar systems are comparable with the sizes of supercluster complexes penetrating the whole SDSS survey volume (Liivamägi et al. 2012). We illustrate this in Fig. 8 where we plot the distribution of Luminous Red Galaxies and their superclusters from SDSS in x, y coordinates (Liivamägi et al. 2012). An eye can connect the centres of superclusters into huge systems across the whole volume under study, in analogy with the largest quasar systems.

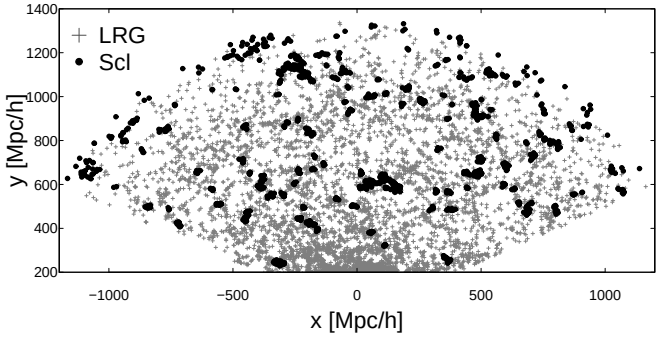

Fig. 8. Distribution of Red Luminous galaxies (light symbols) and their superclusters (dark symbols) in x, y coordinates in a slice of the z-coordinate $-20 \leq z \leq 20$ h^{-1} Mpc.

The mean space density of quasars is approximately $1.1 \cdot 10^{-6}(\mathrm{h^{-1}Mpc})^{-3}$. This is much lower than, for example, the mean space density of nearby galaxy groups in a volume-limited sample with luminosity limit $M_r <= -21.0$, $2 \cdot 10^{-4}(\mathrm{h^{-1}Mpc})^{-3}$, (Tempel et al. 2014). An analysis of the density enhancements around quasars have shown that, in average, quasars can be found in overdense environments, corresponding to small groups or poor (Abell class 0) clusters of galaxies with masses $\approx 10^{12}\mathrm{M_{sun}h^{-1}}$ (Wold et al. 2000; Trainor & Steidel 2012; Shen et al. 2013; Karhunen et al. 2014b; Morselli et al. 2014). The small space density of quasars and mass limit of quasar host haloes tell that quasars are rare events in small groups, rather than common events in rare, very rich clusters (Trainor & Steidel 2012, 2013). A certain fraction of the group-sized haloes undergo short (about 10^7 years, DiPompeo et al. 2014) quasar phase. Different physical processes, which are still not well understood, can trigger a mass flow onto the central super-massive black hole (SMBH) (Portinari et al. 2012; Krumpe et al. 2013).

Fanidakis et al. (2013) showed that in simulations the most luminous quasars do not reside in the most massive dark matter haloes at any redshift. Quasars host haloes have masses typically about $10^{12}\mathrm{M_{sun}h^{-1}}$, it seems to be quite constant as a function of redshift (see also Shen et al. 2013, and references therein). Reason for this is assumed to be AGN feedback mechanism in haloes with $M > 10^{12}\mathrm{M_{sun}h^{-1}}$ (Fanidakis et al. 2013, and references therein). Simulations indicate that at $z = 6$ the very first quasar haloes with mass of $10^{12}\mathrm{M_{sun}h^{-1}}$ are just form-

ing (Heinämäki et al. 2005; Fanidakis et al. 2013). The majority of the descendants of $z = 6$ quasars are located in the haloes which evolve into rich galaxy clusters in the local Universe (Angulo et al. 2012; Fanidakis et al. 2013). At lower redshifts typical quasar host haloes correspond to groups of galaxies.

In the local universe quasars lie in the outskirts of galaxy superclusters (Lietzen et al. 2009, 2011), and in low-density environment a higher fraction of galaxies hosts AGNs than in high-density environment (Kauffmann et al. 2004). The clustering of high-redshift quasars is stronger than the clustering of their low redshift counterparts (Shen et al. 2007).

There are only a few galaxy superclusters known at high redshifts (Nakata et al. 2005; Swinbank et al. 2007; Lubin et al. 2009; Lee et al. 2014). The study of the supercluster Cl 1604 at $z = 0.9$ (Gilbank et al. 2008) showed that AGNs in this supercluster avoid the densest environments (the richest clusters) in the supercluster, being located in intermediate density environments in the supercluster, in the outskirts of massive clusters or within poorer clusters and groups (Kocevski et al. 2009a,b). The quasar from our sample, at $R.A. = 240.27$ degrees, $Dec. = 42.74$ degrees, and redshift $z = 1.05$ may be located in the outskirts of this supercluster.

The quasar systems found in our study may mark the location of galaxy superclusters at high redshifts. The quasars are typically not located in the richest galaxy clusters (in the highest density environments) in superclusters. The mean space density of quasar systems at small linking lengths is of order of $10^{-7}(\mathrm{h}^{-1}\mathrm{Mpc})^{-3}$, this is close to the mean space density of rich superclusters of Abell clusters (Einasto et al. 1997), in support of this suggestion.

5.3. Summary and conclusions

We summarise our results as follows:

1) Quasar systems differ from systems found in a random distribution at the linking lengths $l \leq 30\ h^{-1}$ Mpc, their diameters (up to $30 - 60\ h^{-1}$ Mpc) are comparable to the diameters of poor galaxy superclusters in the local Universe. The richest systems have four member quasars. The mean space density of quasar systems, $\approx 10^{-7}(\mathrm{h}^{-1}\mathrm{Mpc})^{-3}$, is close to the mean space density of local rich superclusters.
2) In a wide linking length interval, $40 \leq l \leq 70\ h^{-1}$ Mpc, the richness and diameters of the richest quasar systems are comparable to those found in random catalogues. The diameters of richest quasar systems ($\approx 200 - 700\ h^{-1}$ Mpc) are comparable to the diameters of rich galaxy superclusters and supercluster chains in the local Universe.
3) Quasar systems begin to join into percolating system at the linking lengths $l \geq 80\ h^{-1}$ Mpc, while in random catalogues the percolation occurs at a larger linking length.
4) At the linking length $l = 70\ h^{-1}$ Mpc three systems from our catalogue coincide with the Large Quasar Groups from Clowes et al. (2012, 2013). At this linking length the largest systems with diameters exceeding $500\ h^{-1}$ Mpc are comparable to the supercluster complexes in the local Universe, penetrating the whole sample volume.

Quasar system catalogues serve as a database to search for distant superclusters of galaxies and to study the cosmic web at high redshifts.

Deeper and wider galaxy surveys are needed to determine quasar's role in the evolution of the large-scale structure of the Universe. We plan to continue our study of quasars and their systems using observational data and simulations to understand better how quasars trace the cosmic web.

Acknowledgments

We thank our referee for comments and suggestions which helped to improve the paper. We are pleased to thank the SDSS Team for the publicly available data releases. Funding for the Sloan Digital Sky Survey (SDSS) and SDSS-II has been provided by the Alfred P. Sloan Foundation, the Participating Institutions, the National Science Foundation, the U.S. Department of Energy, the National Aeronautics and Space Administration, the Japanese Monbukagakusho, and the Max Planck Society, and the Higher Education Funding Council for England. The SDSS Web site is `http://www.sdss.org/`. The SDSS is managed by the Astrophysical Research Consortium (ARC) for the Participating Institutions. The Participating Institutions are the American Museum of Natural History, Astrophysical Institute Potsdam, University of Basel, University of Cambridge, Case Western Reserve University, The University of Chicago, Drexel University, Fermilab, the Institute for Advanced Study, the Japan Participation Group, The Johns Hopkins University, the Joint Institute for Nuclear Astrophysics, the Kavli Institute for Particle Astrophysics and Cosmology, the Korean Scientist Group, the Chinese Academy of Sciences (LAMOST), Los Alamos National Laboratory, the Max-Planck-Institute for Astronomy (MPIA), the Max-Planck-Institute for Astrophysics (MPA), New Mexico State University, Ohio State University, University of Pittsburgh, University of Portsmouth, Princeton University, the United States Naval Observatory, and the University of Washington.

The present study was supported by the Estonian Ministry for Education and Science research project SF0060067s08, by ETAG project IUT26-2, and by the European Structural Funds grant for the Centre of Excellence "Dark Matter in (Astro)particle Physics and Cosmology" TK120. H. Lietzen acknowledges financial support from the Spanish Ministry of Economy and Competitiveness (MINECO) under the 2011 Severo Ochoa Program MINECO SEV-2011-0187. This work has also been supported by ICRAnet through a professorship for Jaan Einasto. C. Park and H. Song thank Korea Institute for Advanced Study for providing computing resources (KIAS Center for Advanced Computation Linux Cluster System).

References

Angulo, R. E., Springel, V., White, S. D. M., et al. 2012, MNRAS, 425, 2722
Chon, G., Böhringer, H., & Nowak, N. 2013, MNRAS, 429, 3272
Clowes, R. G. & Campusano, L. E. 1991, MNRAS, 249, 218
Clowes, R. G., Campusano, L. E., Graham, M. J., & Söchting, I. K. 2012, MNRAS, 419, 556
Clowes, R. G., Harris, K. A., Raghunathan, S., et al. 2013, MNRAS, 429, 2910
Coldwell, G. V. & Lambas, D. G. 2006, MNRAS, 371, 786
Costa-Duarte, M. V., Sodré, Jr., L., & Durret, F. 2011, MNRAS, 411, 1716
DiPompeo, M. A., Myers, A. D., Hickox, R. C., Geach, J. E., & Hainline, K. N. 2014, ArXiv e-prints: 1406.0778
Donoso, E., Li, C., Kauffmann, G., Best, P. N., & Heckman, T. M. 2010, MNRAS, 407, 1078
Dressler, A. 1980, ApJ, 236, 351
Einasto, J. & Gramann, M. 1993, ApJ, 407, 443
Einasto, J., Saar, E., Kaasik, A., & Chernin, A. D. 1974, Nature, 252, 111
Einasto, J., Suhhonenko, I., Hütsi, G., et al. 2011a, A&A, 534, A128
Einasto, M. & Einasto, J. 1987, MNRAS, 226, 543
Einasto, M., Einasto, J., Tago, E., Dalton, G. B., & Andernach, H. 1994, MNRAS, 269, 301
Einasto, M., Einasto, J., Tago, E., Müller, V., & Andernach, H. 2001, AJ, 122, 2222
Einasto, M., Lietzen, H., Tempel, E., et al. 2014, A&A, 562, A87

Einasto, M., Liivamägi, L. J., Tago, E., et al. 2011b, A&A, 532, A5
Einasto, M., Liivamägi, L. J., Tempel, E., et al. 2011c, ApJ, 736, 51
Einasto, M., Tago, E., Jaaniste, J., Einasto, J., & Andernach, H. 1997, A&AS, 123, 119
Eke, V. R., Baugh, C. M., Cole, S., et al. 2004, MNRAS, 348, 866
Falomo, R., Bettoni, D., Karhunen, K., Kotilainen, J. K., & Uslenghi, M. 2014, ArXiv e-prints
Falomo, R., Farina, E. P., Decarli, R., Treves, A., & Kotilainen, J. 2013, in IAU Symposium, Vol. 295, IAU Symposium, ed. D. Thomas, A. Pasquali, & I. Ferreras, 56–56
Fanidakis, N., Macciò, A. V., Baugh, C. M., Lacey, C. G., & Frenk, C. S. 2013, MNRAS, 436, 315
Floyd, D. J. E., Dunlop, J. S., Kukula, M. J., et al. 2013, MNRAS, 429, 2
Gilbank, D. G., Yee, H. K. C., Ellingson, E., et al. 2008, ApJL, 677, L89
Heinämäki, P., Suhhonenko, I., Saar, E., et al. 2005, ArXiv e-print:0507197
Huchra, J. P. & Geller, M. J. 1982, ApJ, 257, 423
Hutchings, J. B., Frenette, D., Hanisch, R., et al. 2002, AJ, 123, 2936
Hutchings, J. B., Scholz, P., & Bianchi, L. 2009, AJ, 137, 3533
Jaaniste, J., Tago, E., Einasto, M., et al. 1998, A&A, 336, 35
Karhunen, K., Kotilainen, J. K., Falomo, R., & Bettoni, D. 2014a, ArXiv e-print: 1404.1642
Karhunen, K., Kotilainen, J. K., Falomo, R., & Bettoni, D. 2014b, MNRAS, 441, 1802
Kauffmann, G., White, S. D. M., Heckman, T. M., et al. 2004, MNRAS, 353, 713
Klypin, A. & Shandarin, S. F. 1993, ApJ, 413, 48
Kocevski, D. D., Lubin, L. M., Gal, R., et al. 2009a, ApJ, 690, 295
Kocevski, D. D., Lubin, L. M., Lemaux, B. C., et al. 2009b, ApJ, 700, 901
Komberg, B. V., Kravtsov, A. V., & Lukash, V. N. 1996, MNRAS, 282, 713
Kotilainen, J., Falomo, R., Bettoni, D., Karhunen, K., & Uslenghi, M. 2013, ArXiv e-print: 1302.1366
Kotilainen, J. K., Falomo, R., Decarli, R., et al. 2009, ApJ, 703, 1663
Krumpe, M., Miyaji, T., & Coil, A. L. 2013, ArXiv e-print: 1308.5976
Lee, K.-S., Dey, A., Hong, S., et al. 2014, ArXiv e-print: 1405.2620
Letawe, Y., Letawe, G., & Magain, P. 2010, MNRAS, 403, 2088
Lietzen, H., Heinämäki, P., Nurmi, P., et al. 2011, A&A, 535, A21
Lietzen, H., Heinämäki, P., Nurmi, P., et al. 2009, A&A, 501, 145
Lietzen, H., Tempel, E., Heinämäki, P., et al. 2012, A&A, 545, A104
Liivamägi, L. J., Tempel, E., & Saar, E. 2012, A&A, 539, A80
Loeb, A. 2008, ArXiv: 0804.2258
Lubin, L. M., Gal, R. R., Lemaux, B. C., Kocevski, D. D., & Squires, G. K. 2009, AJ, 137, 4867
Luparello, H., Lares, M., Lambas, D. G., & Padilla, N. 2011, MNRAS, 415, 964
Martinez, V. J., Pons-Borderia, M.-J., Moyeed, R. A., & Graham, M. J. 1998, MNRAS, 298, 1212
Miller, L., Croom, S. M., Boyle, B. J., et al. 2004, MNRAS, 355, 385
Mo, H. J., Einasto, M., Xia, X. Y., & Deng, Z. G. 1992, MNRAS, 255, 382
Morselli, L., Mignoli, M., Gilli, R., et al. 2014, ArXiv e-print: 1406.3961
Mountrichas, G., Sawangwit, U., Shanks, T., et al. 2009, MNRAS, 394, 2050
Nadathur, S. 2013, MNRAS, 434, 398
Nakata, F., Kodama, T., Shimasaku, K., et al. 2005, MNRAS, 357, 1357
Padmanabhan, N., White, M., Norberg, P., & Porciani, C. 2009, MNRAS, 397, 1862
Park, C., Choi, Y., Vogeley, M. S., Gott, III, J. R., & Blanton, M. R. 2007, ApJ, 658, 898
Park, C. & Choi, Y.-Y. 2009, ApJ, 691, 1828
Park, C., Choi, Y.-Y., Kim, J., et al. 2012, ApJL, 759, L7
Portinari, L., Kotilainen, J., Falomo, R., & Decarli, R. 2012, MNRAS, 420, 732
Richards, G. T., Strauss, M. A., Fan, X., et al. 2006, AJ, 131, 2766
Schirmer, M., Hildebrandt, H., Kuijken, K., & Erben, T. 2011, A&A, 532, A57
Schneider, D. P., Richards, G. T., Hall, P. B., et al. 2010, AJ, 139, 2360
Shen, Y., McBride, C. K., White, M., et al. 2013, ApJ, 778, 98
Shen, Y., Strauss, M. A., Oguri, M., et al. 2007, AJ, 133, 2222
Skibba, R. A. 2009, MNRAS, 392, 1467
Söchting, I. K., Clowes, R. G., & Campusano, L. E. 2004, MNRAS, 347, 1241
Soechting, I. K., Clowes, R. G., & Campusano, L. E. 2002, in Bulletin of the American Astronomical Society, Vol. 34, American Astronomical Society Meeting Abstracts #200, 649
Suhhonenko, I., Einasto, J., Liivamägi, L. J., et al. 2011, A&A, 531, A149
Swinbank, A. M., Edge, A. C., Smail, I., et al. 2007, MNRAS, 379, 1343
Tago, E., Einasto, J., Saar, E., et al. 2006, Astronomische Nachrichten, 327, 365
Tago, E., Einasto, J., Saar, E., et al. 2008, A&A, 479, 927
Tempel, E., Saar, E., Liivamägi, L. J., et al. 2011, A&A, 529, A53
Tempel, E., Tago, E., & Liivamägi, L. J. 2012, A&A, 540, A106
Tempel, E., Tamm, A., Gramann, M., et al. 2014, ArXiv e-print: 1402.1350
Trainor, R. & Steidel, C. C. 2013, ApJL, 775, L3
Trainor, R. F. & Steidel, C. C. 2012, ApJ, 752, 39
Tucker, D. L., Oemler, Jr., A., Hashimoto, Y., et al. 2000, ApJS, 130, 237
Ueda, S., Hayashida, K., Anabuki, N., et al. 2013, ApJ, 778, 33
van de Weygaert, R. & Schaap, W. 2009, in Lecture Notes in Physics, Berlin Springer Verlag, Vol. 665, Data Analysis in Cosmology, ed. V. J. Martínez, E. Saar, E. Martínez-González, & M.-J. Pons-Bordería, 291–413
Vanden Berk, D. E., Schneider, D. P., Richards, G. T., et al. 2005, AJ, 129, 2047
Webster, A. 1982, MNRAS, 199, 683
Williger, G. M., Campusano, L. E., Clowes, R. G., & Graham, M. J. 2002, ApJ, 578, 708
Wold, M., Lacy, M., Lilje, P. B., & Serjeant, S. 2000, MNRAS, 316, 267
Zeldovich, I. B., Einasto, J., & Shandarin, S. F. 1982, Nature, 300, 407

Appendix A: Data on quasar systems

Table A.1. Data on QSO systems with $N_{QSO} = 3$ at linking length 20 h^{-1} Mpc.

(1)	(2)	(3)	(4)	(5)	(6)	(7)	(8)
ID	R.A.	Dec.	λ	η	z	Diameter	N_{70}
	[deg]	[deg]	[deg]	[deg]		[h^{-1} Mpc]	
22	127.99	45.66	-35.88	29.48	1.76	29.9	4
36	132.41	38.17	-38.63	19.79	1.75	22.0	10
53	135.41	8.50	-48.85	-19.51	1.21	31.0	5
124	149.80	22.13	-32.27	-6.04	1.36	17.6	9
161	157.01	5.17	-27.86	-26.63	1.28	16.6	3
166	158.73	52.24	-15.71	22.72	1.38	17.6	3
167	159.08	56.72	-13.87	26.94	1.26	22.7	5
215	166.34	56.22	-10.24	25.13	1.21	21.7	3
251	173.48	19.62	-10.83	-12.49	1.19	14.9	5
272	177.85	57.90	-3.78	25.61	1.19	19.0	9
318	187.09	36.84	1.67	4.36	1.62	22.5	17
350	193.55	37.31	6.79	5.12	1.64	20.9	3
354	194.57	19.71	9.01	-12.53	1.21	18.1	3
366	196.17	24.45	10.15	-7.63	1.72	27.8	5
379	198.68	58.00	7.20	26.23	1.04	29.2	8
415	205.47	60.14	10.02	29.23	1.30	24.2	9
430	207.98	2.79	22.95	-29.46	1.22	11.0	4
435	209.40	62.39	11.03	32.03	1.19	11.1	28
456	213.77	11.32	28.16	-19.62	1.55	13.8	21
472	216.68	36.76	24.88	8.77	1.23	24.9	6
544	235.02	54.57	26.37	32.93	1.65	29.9	14

Notes. Columns are as follows: 1: ID of the system; 2–3: system right ascension and declination; 4–5: system SDSS coordinates λ and η; 6: mean redshift of the system; 7: system size; 8: the richness of a systems to which a given system belongs at the linking length 70 h^{-1} Mpc.

Table A.2. Data on QSO systems with $N_{QSO} = 4$ at linking length 30 h^{-1} Mpc.

(1)	(2)	(3)	(4)	(5)	(6)	(7)	(8)
ID	R.A.	Dec.	λ	η	z	Diameter	N_{70}
	[deg]	[deg]	[deg]	[deg]		[h^{-1} Mpc]	
50	128.06	45.73	-35.79	29.50	1.77	34.97	4
122	135.29	8.64	-48.94	-19.27	1.21	44.55	5
158	137.94	8.32	-46.41	-20.37	1.53	43.11	30
195	140.69	14.19	-42.62	-13.02	1.46	49.47	28
496	162.75	57.62	-11.69	27.09	1.10	36.37	8
501	162.57	15.90	-21.52	-15.36	1.25	38.32	67
657	173.32	19.64	-10.98	-12.47	1.18	37.74	5
721	178.13	57.89	-3.64	25.57	1.19	37.44	9
1135	208.12	2.89	23.09	-29.34	1.22	34.70	4
1182	212.85	58.62	14.07	29.17	1.26	58.89	16
1477	238.18	48.25	32.21	29.36	1.74	44.47	5
1490	239.04	7.08	53.44	-20.55	1.10	34.74	4

Notes. Columns are the same as in Table A.1.

Table A.3. Data on QSO systems with $N_{QSO} \geq 30$ at linking length 70 h^{-1} Mpc.

(1)	(2)	(3)	(4)	(5)	(6)	(7)	(8)	(9)
ID	$N_{\rm QSO}$	R.A.	Dec.	λ	η	z	Diameter	Comments
		[deg]	[deg]	[deg]	[deg]		[h^{-1} Mpc]	
356	30	138.06	7.86	-46.34	-21.09	1.55	346.8	
1044	33	157.76	20.72	-25.33	-9.44	1.59	336.5	
1093	34	161.31	3.86	-23.61	-28.28	1.11	403.5	C3
1156	56	166.95	33.83	-14.86	2.74	1.11	548.3	
1159	31	162.14	5.47	-22.73	-26.55	1.28	389.1	C2
1195	67	163.63	14.56	-20.59	-16.89	1.27	703.1	C1
1593	31	176.48	38.26	-6.66	6.09	1.28	330.5	
1598	32	177.43	32.67	-6.38	0.41	1.18	457.3	
1771	33	183.60	11.03	-1.35	-21.44	1.08	524.5	
2002	36	189.03	44.08	2.86	11.68	1.39	504.6	
2011	37	189.46	20.28	4.18	-12.14	1.46	454.0	
2190	55	196.49	27.06	10.23	-4.93	1.59	614.6	
2203	64	196.42	39.90	8.78	8.00	1.14	536.4	
2287	31	199.49	54.73	8.30	23.16	1.48	381.9	
2440	41	205.31	50.40	12.65	19.76	1.39	554.1	
2454	31	202.67	21.32	16.41	-10.20	1.08	375.2	
2961	30	217.23	10.45	31.63	-20.20	1.68	387.5	
3205	38	227.57	41.44	30.42	17.69	1.54	471.7	
3219	46	226.66	16.73	39.53	-10.59	1.09	470.6	
3323	34	228.51	8.09	42.95	-21.40	1.22	399.9	
3352	43	230.99	47.80	28.84	25.28	1.57	458.7	
3431	34	234.53	10.74	48.33	-16.14	1.24	390.5	

Notes. Columns are as follows: 1: ID of the system; 2: the number of quasars in the system, $N_{\rm QSO}$; 3–4: system right ascension and declination; 5–6: system SDSS coordinates λ and η; 7: mean redshift of the system; 8: system size; 9: comments. C1–C3: large QSO groups, described in: C1–Clowes et al. (2013), C2, C3–Clowes et al. (2012).